



Research paper

Guidelines for FEM modelling of wood-CFRP beams using ABAQUS

Bartosz Kawecki¹

Abstract: The article presents detailed guidelines for the nonlinear modelling of wood–CFRP beams with full cross-section using the Finite Element Method (FEM). Reviewing the literature has shown that behaviour of such composites is a current research topic, undertaken by many scientists. Complex numerical models made in the Simulia ABAQUS software are the basis for modelling recommendations. Properties of the materials consider the orthotropy and plasticity of wood and CFRP tapes, and the stiffness of adhesive layers with delamination. Results of laboratory experiments, got for a statistically significant number of specimens, confirm the model assumptions. This research paper provides a rich source of knowledge and experiences for scientists and engineers, who deal with mechanics of wood–CFRP composites. The uniqueness of the presentation lies in the detailed description of the complex numerical model. Specification comprises the steps necessary to do complete and successful calculations. The model is suitable for analysing the behaviour of wood–CFRP composites in different reinforcement configurations.

Keywords: ABAQUS, FEM, wood–CFRP beams, nonlinear analysis, modelling

¹PhD. Eng., Lublin University of Technology, Faculty of Civil Engineering and Architecture, ul. Nadbystrzycka 40, 20-618 Lublin, Poland, e-mail: b.kawecki@pollub.pl, ORCID: [0000-0001-8134-5956](https://orcid.org/0000-0001-8134-5956)

1. Introduction

Structural elements made of combining wood with FRP composites are the current research topic undertaken by many scientists. There are several known ideas of strengthening and reinforcing solid and glue laminated timber (GLT).

For strengthening solid wood, the first method is gluing strips to the bottom of a girder on the entire cross-section width. Fiorelli [1] carries out studies on beams reinforced with GFRP and CFRP. Kossakowski [2] uses three types of hand-laminated mats: glass, aramid and carbon. Kim [3, 4] examines the beams with an incision in the middle of the span and uses different thicknesses of CFRP laminations. Corradi [5] analyses the uncertainty of the material properties of the girders reinforced with CFRP and GFRP. De Jesus [6] tests two variants of CFRP reinforcement in half and the entire span. The second method is gluing strips to the bottom of the girder, but not on the entire cross-section width. Andor [7] strengthens the beams using CFRP glued in three variants. Borri [8] reinforces half of the beam width with two thicknesses and as angles (Figure 1a–c). Another method is to fold the composite onto the vertical planes of the girders. Rosa Garcia [9, 10] applies the reinforcement using CFRP and BFRP in a U-shaped form. Rescalvo carries out a comparison of different configurations of CFRP reinforcement (Fig. 1a, b, d, e).

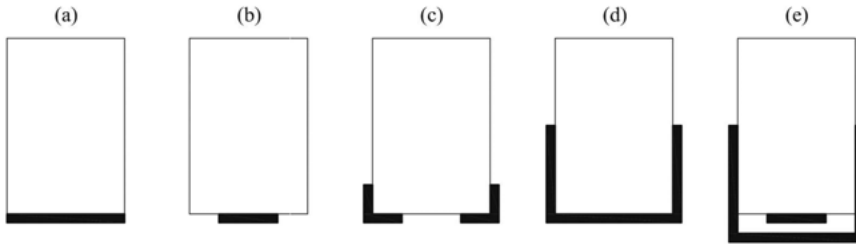


Fig. 1. Methods of strengthening solid wood with FRP outside: a) full-width, b) half-width, c) angles, d) U-shaped, e) cumulative: half-width with U-shaped [11]

The last method is cutting a cross-section and gluing a plate into the prepared incision. Jankowski [12] and Nowak [13] conduct such studies by analysing the configurations shown in Fig. 2a–c. Schober [14] adds reinforcements in two other configurations Fig. 2d, e.

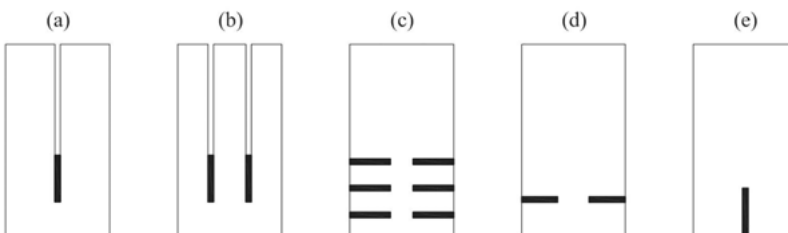


Fig. 2. Methods of strengthening solid wood with FRP in incisions: a) one-internal vertical, b) two-internal vertical, c) six-edge horizontal, d) two-edge – horizontal, e) one-edge vertical [11]

For strengthening glue laminated timber, the first method is to fix FRP to the bottom of a beam. It is the same solution as for solid timber. Vahedian [15] considers different thicknesses of the strips. Thorhallsson [16] reinforces GLT using GFRP and BFRP. Brunetti [17] uses two different glues and different thicknesses of reinforcements. Glisovic [18, 19] tests glued laminated timber reinforced with CFRP in various configurations (Fig. 1b and 2d, e), while Subhani [20] in two other variants (Fig. 1a, d). Fiorelli [21] and Raftery [22–24] do laboratory tests and statistical analyses of the results (Fig. 3a). Osmannezhad [25] proposes gluing GFRP between the layers of GLT in various configurations as shown in Fig. 3b, c. Shi [26] glues GFRP into each joint of GLT and then around the perimeter of the beam cross-section as shown in Fig. 3d.

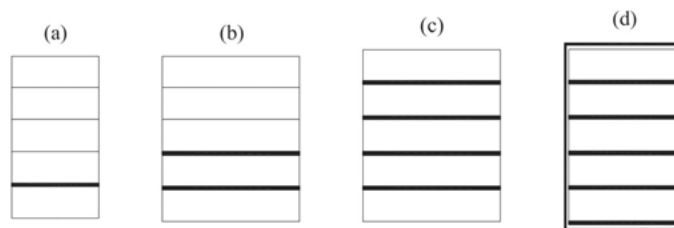


Fig. 3. Methods of strengthening solid wood with FRP in different configurations: a) one strip, b) two strips, c) four strips, d) four strips and around the perimeter [11]

A few studies present the attempts to model the beam elements, but they do not give enough details to recreate the models using the same software. This causes difficulties for researchers or engineers to solve a similar problem using the models. Nowak [13] conducts FE modelling on the beams presented in Fig. 2a–c. Glisovic [27], proposes FE modelling of beams tested in his earlier work [18, 19]. The model is similar to this performed by Nowak [13] and Khelifa [28]. Raftery [23] performs FE modelling based on the assumptions in the papers of Nowak [13], Glisovic [27] and Khelifa [28]. The author of the paper proposes a well-described model suitable for many applications.

2. Laboratory tests and FEM model validation

The author of the paper performs laboratory tests in the four point bending setup shown in Fig. 4. The entire length of the beam is 2000 mm, bottom supports span is $L = 1800$ mm and cross-section average dimensions are BW (93.5×160.8 mm) and BWW (93.3×162.1 mm). The number of the tested specimens is 7 pieces per each configuration (Fig. 5). Painting samples with a special stochastic pattern enables to use a Digital Image Correlation (DIC) method to see damage in the beams (only in the middle of the sample, because the machine columns block the view).

Fig. 6 shows modelling techniques and general assumptions. Then, Fig. 7 presents a comparison of the numerical simulations results. Crack of the lowest wooden lamella determines the limit force value (P_{\max}) – the analysis does not continue further.

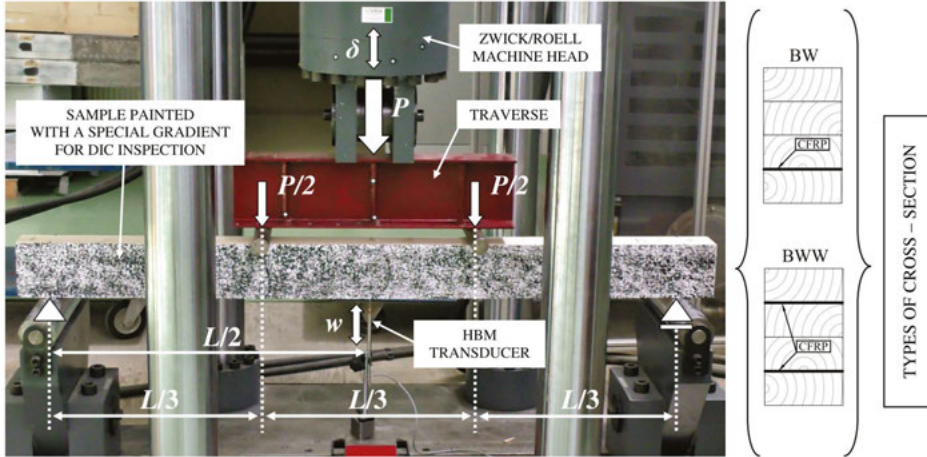


Fig. 4. Laboratory setup

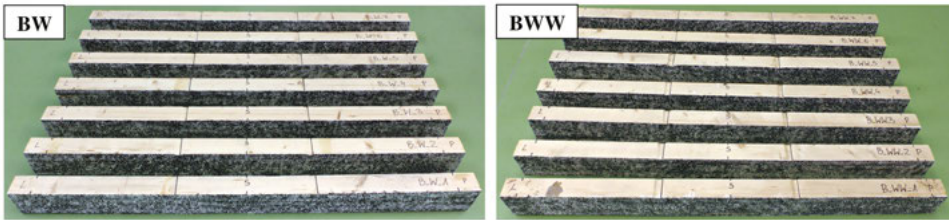


Fig. 5. Specimens after the experimental tests

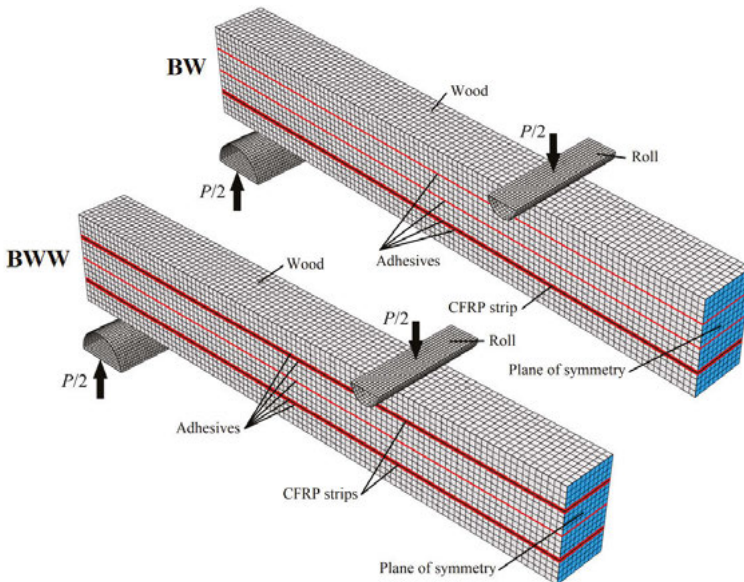


Fig. 6. General assumptions of the FEM models

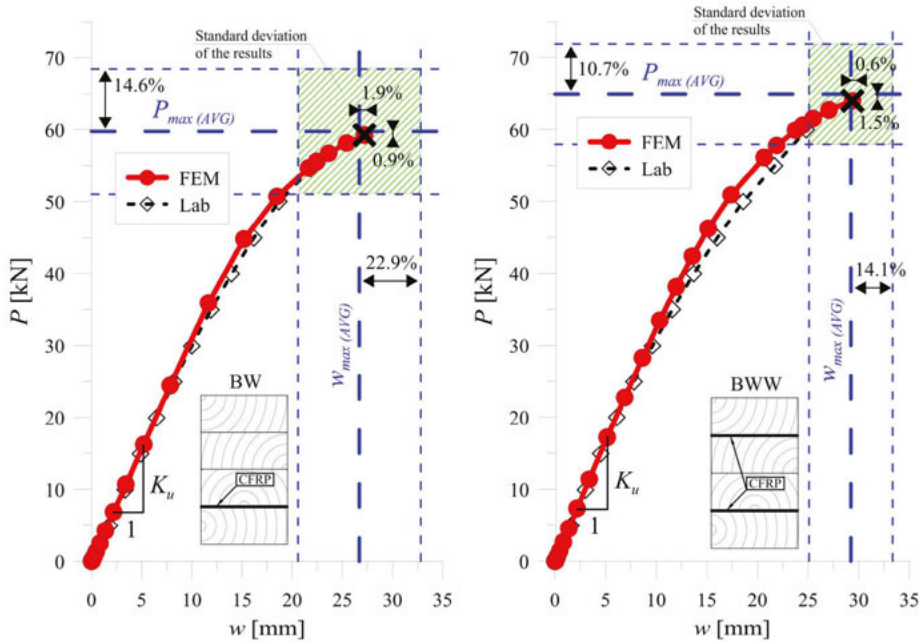


Fig. 7. Comparison of the FEM results to the laboratory tests

In the laboratory experiments, *BW* samples show scatter of results on a level of 14.6% for P_{max} and 22.9% for w_{max} , while *BWW* samples 10.7% for P_{max} and 14.1% for w_{max} , which is normal for wood members. The error in predicting the average maximum values (P_{max} , w_{max}) with the numerical model is less than 2% and P/w path is very close to the experimental average path. It proves a high accuracy of the FEM simulations.

The other steps made to confirm the model are comparing the regions that have become plasticised (Fig. 8) and analysing damage patterns (Fig. 9–12) of two exemplary *BW* and *BWW*

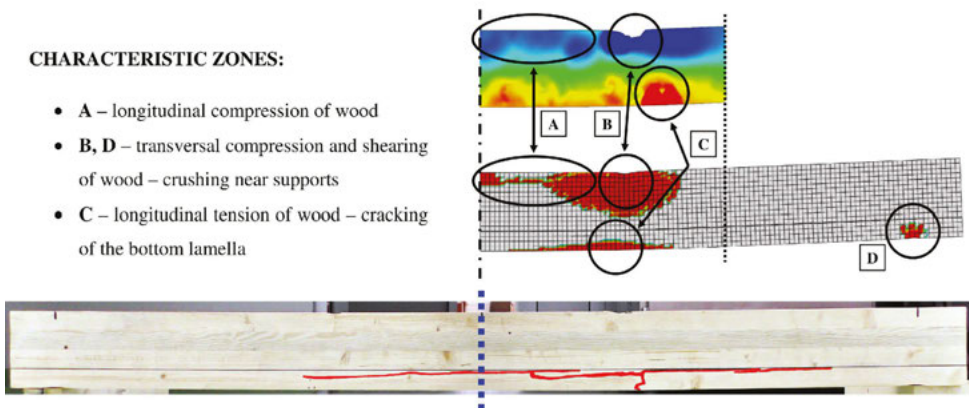


Fig. 8. FEM – DIC comparison and exemplary crack of the bottom lamella

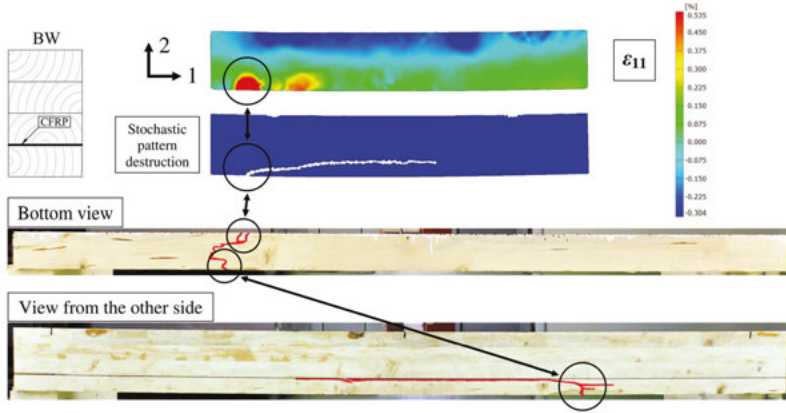


Fig. 9. 1st example of damage pattern for *BW* sample

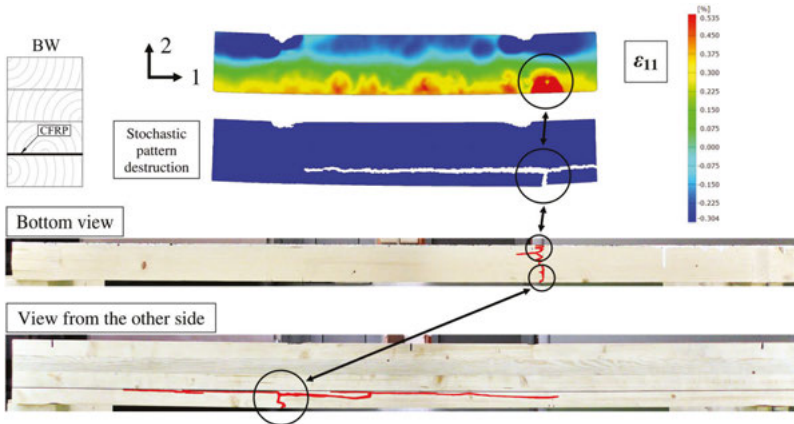


Fig. 10. 2nd example of damage pattern for *BW* sample

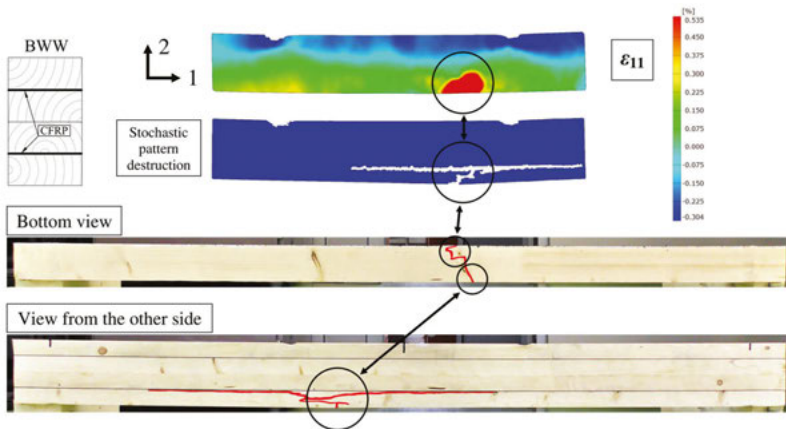


Fig. 11. 1st example of damage pattern for *BWW* sample

samples in details. The modes of failure in FEM simulations are similar to these obtained in laboratory tests for all of the presented examples. This acknowledges the correctness of the model assumptions.

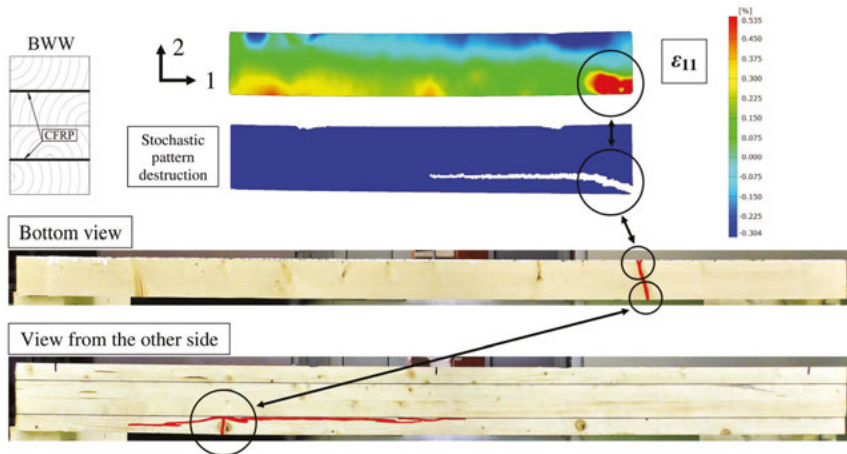


Fig. 12. 2nd example of damage pattern for *BWW* sample

3. FEM model creation – detailed description

This section is unique comparing to the papers with FEM modelling published in other journals, because it describes how to create the model step by step. It can simplify the path for researchers or engineers to solve a similar problem using the model. A *BW* configuration is the example for detailed description of the modelling techniques, because it has fewer elements than *BWW*. The chapter presents the used algorithm and choice of material properties.

Crucial information is that oneself does not set the units in the Simulia ABAQUS software, but should define and remember them by himself at every stage of creating the model.

3.1. Parts

The first stage is creating separate parts for wood lamellas, adhesive layers, CFRP tapes and machine rolls. The entire length of the beam is 2000 mm and width 93.5 mm – each beam part is the same length and every of them is *3D/Deformable/Solid/Extrusion*. Single wood lamella height is 39.75 mm, single adhesive layer – 0.1 mm and CFRP tape – 1.4 mm. Machine rolls are not a part of the beam, but they belong to the laboratory setup. Diameter of the bottom roll is 100 mm and top roll – 50 mm – defined as *3D/Discrete rigid/Shell/Extrusion*. Adding reference points (*RP*) simplify the control of boundary conditions and loads. Wood-adhesive layers should be a separate part from wood-CFRP adhesives, because properties of the layers may be different. Sketching the parts is a trivial skill, and for more information the reader should look at the ABAQUS User's Guide [29].

3.2. Materials

The second stage is creating materials definition, different for each part. Preparing two separate materials for wood and CFRP in compression and tension is necessary – it enables to distinguish between compressive (f_c) and tensile (f_t) strength [30] (Fig. 13).

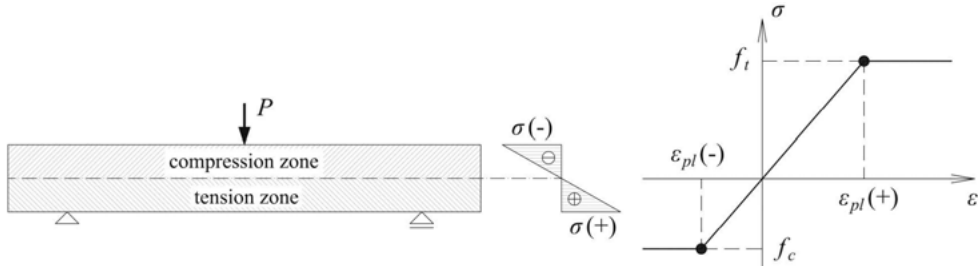


Fig. 13. Dividing beam into compression/tension zone and constitutive law for wood [30]

Material of wood and CFRP tapes is *Elastic/Engineering Constants* and *Plastic/Isotropic with Potential*. Then one can set the proper material properties – elastic modules: E_1, E_2, E_3 , Poisson ratios: $\nu_{12}, \nu_{13}, \nu_{23}$ and shear modules: G_{12}, G_{13}, G_{23} . Adding *Potential* option enables to define strength in respective directions using Hill's function coefficients: $R_{11}, R_{22}, R_{33}, R_{12}, R_{13}, R_{23}$. Table 1 presents the set values and Fig. 14 shows the order of entering the properties to the Simulia ABAQUS software.

Table 1. Properties of wood and CFRP tapes

Parameter	Wood	CFRP tape
E_1 [GPa]	11.439	175.000
E_2 [GPa]	0.732	7.100
E_3 [GPa]	0.458	
ν_{12} [/]	0.335	
ν_{13} [/]	0.358	0.300
ν_{23} [/]	0.416	
G_{12} [GPa]	0.715	2.730
G_{13} [GPa]	0.529	
G_{23} [GPa]	0.069	
f [MPa]	61.17	2800.00
$R_{11}(+)$ [/]	0.680	1.000
$R_{11}(-)$ [/]	0.484	0.025
$R_{22} = R_{33}$ [/]	0.061	0.025
$R_{12} = R_{13} = R_{23}$ [/]	0.206	0.016

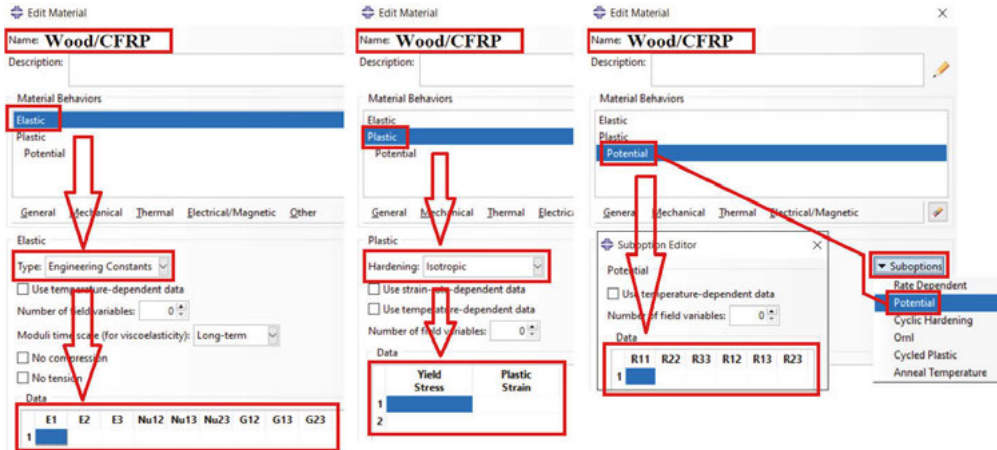


Fig. 14. Editing material properties – Wood–CFRP

Material of adhesive layers is *Elastic/Traction* and *Quads Damage*. The described example assumes properties for polyurethane (PUR) glue. Fig. 15 shows a constitutive law for the material. Fig. 16 informs how to set the proper material properties. The author states that the wood–wood and wood–CFRP joint stiffness and strength can differ from each other [11]. Adhesive material stiffness has a confusing denotation in the Simulia ABAQUS software. Its correct explanation is: $K_{nn} = E/E_{nn}$ (mode I), $K_{ss} = G_1/E_{ss}$ (mode II), $K_{tt} = G_2/E_{tt}$ (mode III).

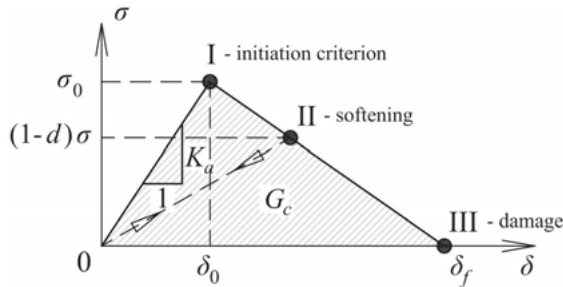


Fig. 15. Constitutive law for adhesive

Formula (3.1) gives the values of each stiffness for wood–wood ($K_{a,K}$) and formula (3.2) for wood–CFRP ($K_{a,KW}$) connection.

$$(3.1) \quad K_{a,K} = K_{nn} = K_{ss} = K_{tt} = 91.32 \text{ MPa/mm}$$

$$(3.2) \quad K_{a,KW} = K_{nn} = K_{ss} = K_{tt} = 49.51 \text{ MPa/mm}$$

Quads Damage choice enables to use a quadratic criterion for damage initiation (3.3). Formula (3.4) gives the values of damage initiation stress in respective directions for wood–

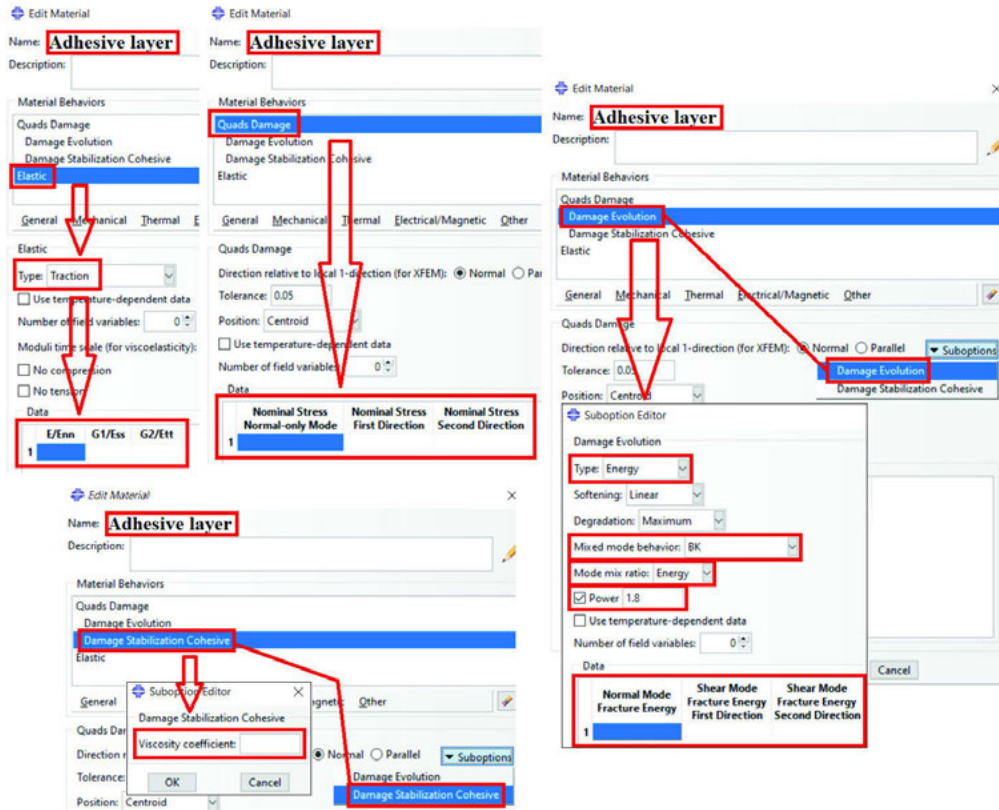


Fig. 16. Editing material properties – Adhesive layer

wood and formula (3.5) for wood–CFRP connection, calculated based on Turon [31].

$$(3.3) \quad \left(\frac{\sigma_{33}}{\sigma_{Ic}} \right)^2 + \left(\frac{\tau_{13}}{\tau_{IIc}} \right)^2 + \left(\frac{\tau_{23}}{\tau_{IIIc}} \right)^2 = 1$$

$$(3.4) \quad \text{wood–wood:} \quad \sigma_{Ic} = 3.19 \text{ MPa}, \quad \tau_{IIc} = \tau_{IIIc} = 9.92 \text{ MPa}$$

$$(3.5) \quad \text{wood–CFRP:} \quad \sigma_{Ic} = 2.23 \text{ MPa}, \quad \tau_{IIc} = \tau_{IIIc} = 6.94 \text{ MPa}$$

To describe progressive delamination, one can use displacement or energy based approach – *Suboptions/Damage Evolution*. In case of this paper the author use *BK* energy based criterion (3.6), determined by Benzeggagh [32]. Formula (3.7) gives the values of energy release rate in respective directions for wood–wood and formula (3.8) for wood–CFRP connection, assumed and assessed based on Xu [33].

$$(3.6) \quad G_c = G_{Ic} + (G_{IIc} - G_{Ic}) \left(\frac{G_{II} + G_{III}}{G_I + G_{II} + G_{III}} \right)^\eta, \quad \eta = 1.8$$

$$(3.7) \quad G_{Ic} = 85 \text{ J/m}^2, \quad G_{IIc} = G_{IIIc} = 820 \text{ J/m}^2$$

$$(3.8) \quad G_{Ic} = 42 \text{ J/m}^2, \quad G_{IIc} = G_{IIIc} = 402 \text{ J/m}^2$$

It is important to set a viscosity coefficient to stabilise the material in a softening regime – *Suboptions/Damage Stabilization Cohesive*. Demir [34] has performed a detailed analysis of the influence of viscosity coefficient on the results. The best value is $\chi = 0.0005$.

Rigid parts as rolls do not have any material properties, because they are non-deformable from their definition.

3.3. Sections

The third stage is creating sections corresponding to the material. The best way is creating section which correspond to the materials defined in an earlier point. It reduces the risk of assigning incorrect material properties to the model.

For wood and CFRP, section is *Solid/Homogenous* and for adhesive layers *Other/Cohesive*. Then in *Cohesive section* the choice is *Response – Traction Separation, Initial thickness – use analysis default* (it provides using basic assumption for cohesive elements and traction separation rules – a unity thickness) – Fig. 17.

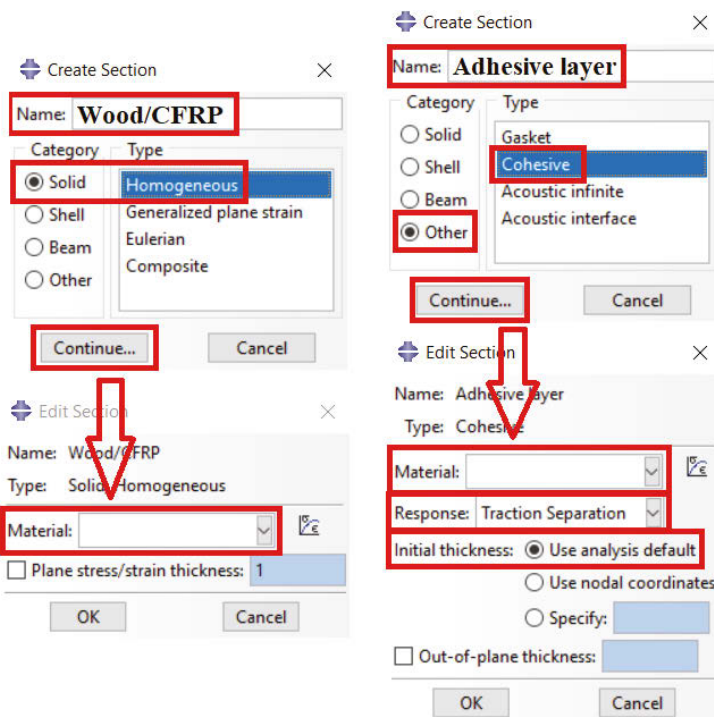


Fig. 17. Creating sections in the FEM model

3.4. Materials' orientation

The fourth stage is assigning the proper orientation of the material to each part. It is necessary and very important to do this step, because the model uses materials with original properties in respective directions – skipping this or setting inappropriate material orientation lead to an error in the very early stage of the analysis. Fig. 18 shows the material orientation for wood, CFRP tape and adhesive layer, corresponding to the materials' properties determined in Section 3.2. The axes 1, 2 and 3 represent axes X, Y and Z in the Simulia ABAQUS software. The best way is to create a new local coordinate system for each part. Creating local coordinate systems and assigning orientations based on them is a trivial skill, and for more information the reader should look at the ABAQUS User's Guide [29].

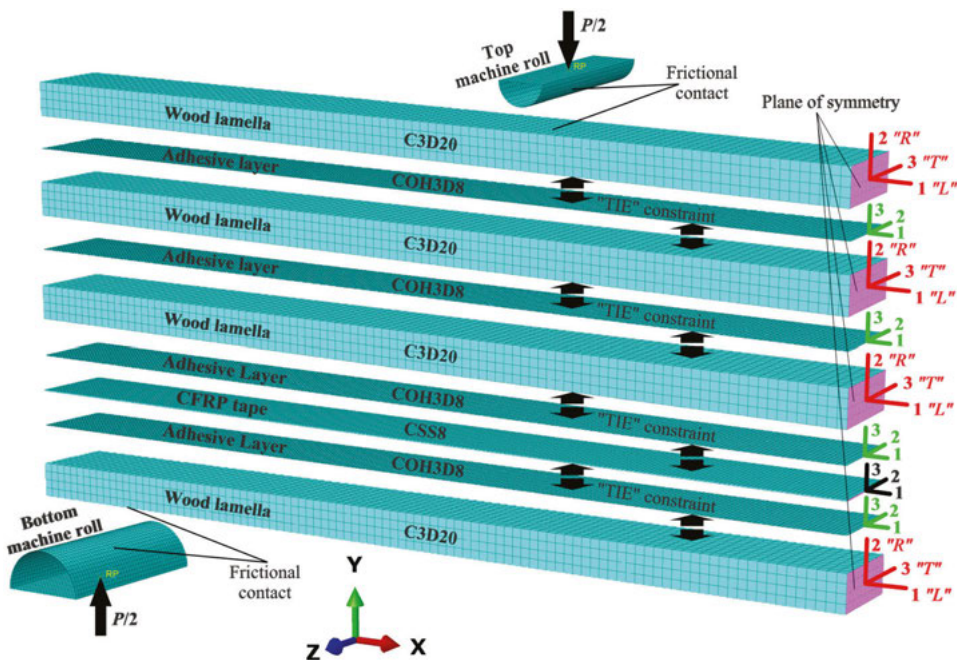


Fig. 18. Assembling the FEM model

3.5. Assembling the model

The fifth stage is assembling the model by defining constraints, interactions and boundary conditions, according to Fig. 18. Constraints, interactions and boundary conditions propagate to the next steps, after assigning them in the initial step. The only way to connect adhesives layers with other elements is *TIE* constraint. It is very important to set the surface of adhesive layer always as “*slave*” and the surfaces of glued components as “*master*”. Setting it the other way round may cause errors or inappropriate processing of delamination. Friction coefficient depends on the specifics of the measuring setup – in the paper it is only a small value ensuring a boundary condition and adjusting the model to the experimental data. The other set is a gen-

eral contact between elements remaining in contact in case of adhesives delamination. Next step is defining boundary conditions (*BC*). Reference points (*RP*) on the rolls are the points to use *Encastre* boundary condition. Adding *X* symmetry (*Symmetry/XSYMM*) to the plane of symmetry (Fig. 18) allows to model only a half of the beam. It ensures a better stability of the model and reduces the number of finite elements, which speeds up the calculations. Sometimes, when frictional contact between rolls and wood lamella has a small value, it may be necessary to block a displacement degree of freedom in *Z* direction in one neutral place of the model.

3.6. Mesh

The sixth stage is meshing parts and setting the stack direction. Presented FEM model considers mesh type and size validated through laboratory experiments. The author reserves that using a different one requires performing separate tests. Mesh is quadrilateral and has the properties:

- Wood lamellas – about $10 \times 10 \times 10$ mm – C3D20 (20-node quadratic brick element), tested by Hemanth [35]. They work well in case of concentrated loads, bending and shearing. Four elements of a height of a cross-section ensures getting exact results.
- Adhesive layers – about $5 \times 5 \times 0.1$ mm – COH3D8 (8-node three-dimensional cohesive element), proposed by Camanho [36]. They allow including stiffness of the adhesive layer and to predict a delamination progress.
- CFRP tapes – about $5 \times 5 \times 1.4$ mm – CSS8 (8-node solid shell element) proposed by Vu-Quoc [37]. They enable modelling shells in a three-dimensional space.
- Machine rolls – about 5×5 mm – R3D4 (4-node 3D rigid quadrilateral element).

It is necessary to indicate stack direction for every part of the model in *Mesh* module – *Mesh/Orientation/Stack*. Directing the composite folding is important, because the Simulia ABAQUS software assigns a random surface by default. It should be always the surface next to the adjacent element. Otherwise, an error or non-physical behaviour of the composite will occur.

3.7. Steps

The seventh stage is creating a loading step and choosing the way of loading. *Time period* should be equal to 1, *Nlgeom* should be active – it ensures considering each of the nonlinearities. An unnecessary choice is the *Automatic stabilization*, which may generate artificial and uncontrolled effects. *Incrementation* type should be *Automatic*. *Increment size* should be small enough to detect a contact at the analysis start. Increasing the *maximum number of increments*, relating to a default value, gives an opportunity to do longer analysis in case of many iterations. The *maximum increment size* depends on the expectations of results density. Fig. 19 presents the proposed values.

A reference point enables to simplify adding a force or a displacement to the construction. Otherwise, it allows you to check these values at the same point during the analysis. Choosing *Loads* in the modelling tree is a way to add a force, while boundary condition is a way to add a displacement. In principle, displacement controlled analysis is easier converging. Many non-linear effects cause the need to increase the allowable number of iterations. A default options

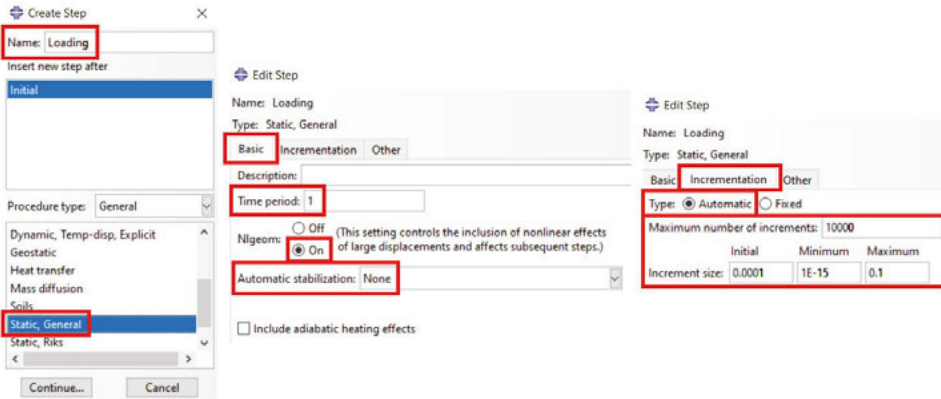


Fig. 19. Creating loading step in the FEM model

in the Simulia ABAQUS software are too small to solve such complex task. We go to *Step* module, choose *Other/General Solution Controls/Manager* and edit loading step, as shown in Fig. 20.

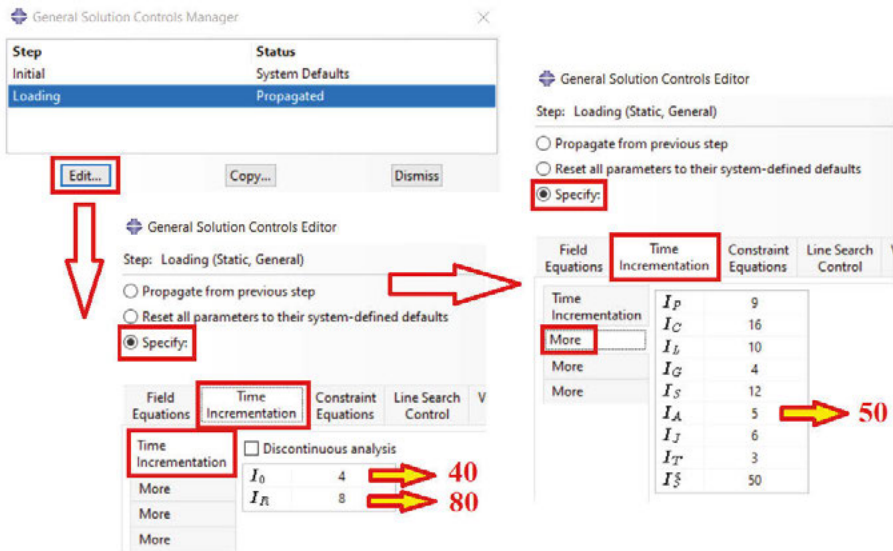


Fig. 20. Controlling solution convergence

3.8. Analysis

The last stage is creating the Job and starting the analysis. It may turn out that a valuable solution is setting *Parallelization* options, when the model is large and the computing station is powerful enough. After performing the described stages, one can start the calculations.

4. Conclusions

The paper presents detailed guidelines for the nonlinear modelling of Wood-CFRP beams with full cross-section using the Finite Element Method (FEM). Complex numerical models made in the Simulia ABAQUS software are the basis for modelling recommendations. Properties of the materials consider the orthotropy and plasticity of wood and CFRP tapes, and the stiffness of adhesive layers with delamination. Results of laboratory experiments, got for a statistically significant number of specimens, confirm the model assumptions. This research paper provides a rich source of knowledge and experiences for scientists and engineers, who deal with mechanics of wood-CFRP composites. The uniqueness of the presentation lies in the detailed description of the complex numerical model. Specification comprises the steps necessary to do complete and successful calculations. The model is suitable for analysing the behaviour of wood-CFRP composites in different reinforcement configurations.

Acknowledgements

The research was done in Lublin University of Technology and funded under the grant “Subvention for Science” (MEiN), Project no. FN-5/2021.

References

- [1] J. Fiorelli and A.A. Dias, “Analysis of the strength and stiffness of timber beams reinforced with carbon fiber and glass fiber”, *Materials Research*, vol. 6, no. 2, pp. 193–202, 2003, DOI: [10.1590/S1516-14392003000200014](https://doi.org/10.1590/S1516-14392003000200014).
- [2] P.G. Kossakowski, “Load – Bearing Capacity of Wooden Beams Reinforced with Composite Sheets”, *Structure*, pp. 1–9, 2011.
- [3] Y.J. Kim and K. A. Harries, “Modeling of timber beams strengthened with various CFRP composites”, *Engineering Structures*, vol. 32, no. 10, pp. 3225–3234, 2010, DOI: [10.1016/j.engstruct.2010.06.011](https://doi.org/10.1016/j.engstruct.2010.06.011).
- [4] Y.J. Kim, M. Hossain, and K.A. Harries, “CFRP strengthening of timber beams recovered from a 32-year old quonset: Element and system level tests”, *Engineering Structures*, vol. 57, pp. 213–221, 2013, DOI: [10.1016/j.engstruct.2013.09.028](https://doi.org/10.1016/j.engstruct.2013.09.028).
- [5] M. Corradi et al., “Uncertainty analysis of FRP reinforced timber beams”, *Composites Part B: Engineering*, vol. 113, pp. 174–184, 2017, DOI: [10.1016/j.compositesb.2017.01.030](https://doi.org/10.1016/j.compositesb.2017.01.030).
- [6] A.M.P. de Jesus, J.M.T. Pinto, and J.J.L. Morais, “Analysis of solid wood beams strengthened with CFRP laminates of distinct lengths”, *Construction and Building Materials*, vol. 35, pp. 817–828, 2012, DOI: [10.1016/j.conbuildmat.2012.04.124](https://doi.org/10.1016/j.conbuildmat.2012.04.124).
- [7] K. Andor et al., “Experimental and statistical analysis of spruce timber beams reinforced with CFRP fabric”, *Construction and Building Materials*, vol. 99, pp. 200–207, 2015, DOI: [10.1016/j.conbuildmat.2015.09.026](https://doi.org/10.1016/j.conbuildmat.2015.09.026).
- [8] A. Borri, M. Corradi, and A. Grazini, “A method for flexural reinforcement of old wood beams with CFRP materials”, *Composites Part B: Engineering*, vol. 36, no. 2, pp. 143–153, 2005, DOI: [10.1016/j.compositesb.2004.04.013](https://doi.org/10.1016/j.compositesb.2004.04.013).
- [9] P. de la Rosa García et al., “Bending reinforcement of timber beams with composite carbon fiber and basalt fiber materials”, *Composites, Part B: Engineering*, vol. 55, pp. 528–536, 2013, DOI: [10.1016/j.compositesb.2013.07.016](https://doi.org/10.1016/j.compositesb.2013.07.016).
- [10] P. de la Rosa García, A. Cobo Escamilla, and M.N. González García, “Analysis of the flexural stiffness of timber beams reinforced with carbon and basalt composite materials”, *Composites, Part B: Engineering*, vol. 86, pp. 152–159, 2016, DOI: [10.1016/j.compositesb.2015.10.003](https://doi.org/10.1016/j.compositesb.2015.10.003).
- [11] B. Kawecki and J. Podgórski, “The Effect of Glue Cohesive Stiffness on the Elastic Performance of Bent Wood-CFRP Beams”, *Materials*, vol. 13, no. 22, pp. 1–23, 2020, DOI: [10.3390/ma13225075](https://doi.org/10.3390/ma13225075).

- [12] L.J. Jankowski, J. Jasięńko, and T.P. Nowak, “Experimental assessment of CFRP reinforced wooden beams by 4-point bending tests and photoelastic coating technique”, *Materials and Structures*, vol. 43, no. 1–2, pp. 141–150, 2010, DOI: [10.1617/s11527-009-9476-0](https://doi.org/10.1617/s11527-009-9476-0).
- [13] T.P. Nowak, J. Jasięńko, and D. Czepiżak, “Experimental tests and numerical analysis of historic bent timber elements reinforced with CFRP strips”, *Construction and Building Materials*, vol. 40, pp. 197–206, 2013, DOI: [10.1016/j.conbuildmat.2012.09.106](https://doi.org/10.1016/j.conbuildmat.2012.09.106).
- [14] K.U. Schober and K. Rautenstrauch, “Post-strengthening of timber structures with CFRP’s”, *Materials and Structures*, vol. 40, no. 1, pp. 27–35, 2007, DOI: [10.1617/s11527-006-9128-6](https://doi.org/10.1617/s11527-006-9128-6).
- [15] A. Vahedian, R. Shrestha, and K. Crews, “Experimental and analytical investigation on CFRP strengthened glulam laminated timber beams: Full-scale experiments”, *Composites Part B: Engineering*, vol. 164, pp. 377–389, 2019, DOI: [10.1016/j.compositesb.2018.12.007](https://doi.org/10.1016/j.compositesb.2018.12.007).
- [16] E.R. Thorhallsson, G.I. Hinriksson, and J.T. Snćbjörnsson, “Strength and stiffness of glulam beams reinforced with glass and basalt fibres”, *Composites Part B: Engineering*, vol. 115, pp. 300–307, 2017, DOI: [10.1016/j.compositesb.2016.09.074](https://doi.org/10.1016/j.compositesb.2016.09.074).
- [17] M. Brunetti et al., “Production feasibility and performance of carbon fibre reinforced glulam beams manufactured with polyurethane adhesive”, *Composites Part B: Engineering*, vol. 156, pp. 212–219, 2019, DOI: [10.1016/j.compositesb.2018.08.075](https://doi.org/10.1016/j.compositesb.2018.08.075).
- [18] I. Glišović et al., “Glulam beams externally reinforced with CFRP plates”, *Wood Research*, vol. 61, no. 1, pp. 141–154, 2016.
- [19] I. Glišović, B. Stevanović, and M. Todorović, “Flexural reinforcement of glulam beams with CFRP plates”, *Materials and Structures*, vol. 49, no. 7, pp. 2841–2855, 2016, DOI: [10.1617/s11527-015-0690-7](https://doi.org/10.1617/s11527-015-0690-7).
- [20] M. Subhani, A. Globa, R. Al-Ameri, and J. Moloney, “Flexural strengthening of LVL beam using CFRP”, *Construction and Building Materials*, vol. 150, pp. 480–489, 2017, DOI: [10.1016/j.conbuildmat.2017.06.027](https://doi.org/10.1016/j.conbuildmat.2017.06.027).
- [21] J. Fiorelli and A.A. Dias, “Glulam beams reinforced with FRP externally-bonded: theoretical and experimental evaluation”, *Materials and Structures*, vol. 44, no. 8, pp. 1431–1440, 2011, DOI: [10.1617/s11527-011-9708-y](https://doi.org/10.1617/s11527-011-9708-y).
- [22] G.M. Raftery and A.M. Harte, “Low-grade glued laminated timber reinforced with FRP plate”, *Composites Part B: Engineering*, vol. 42, no. 4, pp. 724–735, 2011, DOI: [10.1016/j.compositesb.2011.01.029](https://doi.org/10.1016/j.compositesb.2011.01.029).
- [23] G.M. Raftery and A.M. Harte, “Nonlinear numerical modelling of FRP reinforced glued laminated timber”, *Composites Part B: Engineering*, vol. 52, pp. 40–50, 2013, DOI: [10.1016/j.compositesb.2013.03.038](https://doi.org/10.1016/j.compositesb.2013.03.038).
- [24] G.M. Raftery and P.D. Rodd, “FRP reinforcement of low-grade glulam timber bonded with wood adhesive”, *Construction and Building Materials*, vol. 91, pp. 116–125, 2015, DOI: [10.1016/j.conbuildmat.2015.05.026](https://doi.org/10.1016/j.conbuildmat.2015.05.026).
- [25] S. Osmannezhad, M. Faezipour, and G. Ebrahimi, “Effects of GFRP on bending strength of glulam made of poplar (*Populus deltoids*) and beech (*Fagus orientalis*)”, *Construction and Building Materials*, vol. 51, pp. 34–39, 2014, DOI: [10.1016/j.conbuildmat.2013.10.035](https://doi.org/10.1016/j.conbuildmat.2013.10.035).
- [26] H. Shi et al., “Flexural responses and pseudo-ductile performance of lattice-web reinforced GFRP-wood sandwich beams”, *Composites Part B: Engineering*, vol. 108, pp. 364–376, 2017, DOI: [10.1016/j.compositesb.2016.10.009](https://doi.org/10.1016/j.compositesb.2016.10.009).
- [27] I. Glišović et al., “Numerical analysis of glulam beams reinforced with CFRP plates”, *Journal of Civil Engineering and Management*, vol. 23, no. 7, pp. 868–879, 2017, DOI: [10.3846/13923730.2017.1341953](https://doi.org/10.3846/13923730.2017.1341953).
- [28] M. Khelifa et al., “Finite element analysis of flexural strengthening of timber beams with Carbon Fibre-Reinforced Polymers”, *Engineering Structures*, vol. 101, pp. 364–375, 2015, DOI: [10.1016/j.engstruct.2015.07.046](https://doi.org/10.1016/j.engstruct.2015.07.046).
- [29] Simulia ABAQUS, User’s Guide, 2019.
- [30] B. Kaweck and J. Podgórski, “3D ABAQUS simulation of bent softwood elements”, *Archives of Civil Engineering*, vol. 66, no. 3, pp. 323–337, 2020, DOI: [10.24425/ace.2020.134400](https://doi.org/10.24425/ace.2020.134400).
- [31] A. Turon et al., “An engineering solution for mesh size effects in the simulation of delamination using cohesive zone models”, *Engineering Fracture Mechanics*, vol. 74, no. 10, pp. 1665–1682, 2007, DOI: [10.1016/j.engfracmech.2006.08.025](https://doi.org/10.1016/j.engfracmech.2006.08.025).
- [32] M.L. Benzeggagh and M. Kenane, “Measurement of mixed-mode delamination fracture toughness of unidirectional glass/epoxy composites with mixed-mode bending apparatus”, *Composites Science and Technology*, vol. 56, pp. 439–449, 1996, DOI: [10.1016/0266-3538\(96\)00005-X](https://doi.org/10.1016/0266-3538(96)00005-X).
- [33] B.H. Xu et al., “Fracture toughnesses of interlaminar fracture of glued-laminated timber”, *Wood Research*, vol. 61, no. 6, pp. 951–958, 2016.

- [34] A. Demir et al., “Effect of viscosity parameter on the numerical simulation of reinforced concrete deep beam behavior”, *The Online Journal of Science and Technology*, vol. 8, no. 3, pp. 50–56, 2018.
- [35] R.H. Hemanth et al., “Performance evaluation of finite elements for analysis of advanced hybrid laminates”, in *ABAQUS User’s Conference*, pp. 1–15, 2010.
- [36] P.P. Camanho et al., “Numerical simulation of mixed-mode progressive delamination in composite materials”, *Journal of Composite Materials*, vol. 37, no. 16, pp. 1415–1438, 2003, DOI: [10.1177/0021998303034505](https://doi.org/10.1177/0021998303034505).
- [37] L. Vu-Quoc and X.G. Tan, “Optimal solid shells for non-linear analyses of multilayer composites. I. Statics”, *Computer Methods in Applied Mechanics and Engineering*, vol. 192, no. 9–10, pp. 975–1016, 2003, DOI: [10.1016/S0045-7825\(02\)00435-8](https://doi.org/10.1016/S0045-7825(02)00435-8).

Wytyczne do modelowania mes belek drewno-CFRP z wykorzystaniem programu ABAQUS

Słowa kluczowe: ABAQUS, MES, belki drewno-CFRP, analiza nieliniowa, wytyczne do modelowania

Streszczenie:

Artykuł przedstawia szczegółowe wytyczne do nieliniowego modelowania belek o pełnym przekroju wykonanych z kompozytu drewno-CFRP z wykorzystaniem Metody Elementów Skończonych (MES). Przegląd literatury pokazał, że zachowanie takich kompozytów jest aktualnym tematem badawczym, podejmowanym przez wielu naukowców. Podstawą zaproponowanych rekomendacji są złożone modele numeryczne wykonane w programie Simulia ABAQUS. Parametry materiałowe uwzględniają ortotropię plastyczność drewna i taśm CFRP, jak również sztywność warstw klejowych i możliwość ich delaminacji. Założenia modelu zostały potwierdzone badaniami laboratoryjnymi przeprowadzonymi na ważnej statystycznie liczbie próbek. Powyższe opracowanie zapewnia bogate źródło wiedzy i doświadczeń dla inżynierów i naukowców zajmujących się mechaniką kompozytów drewno-CFRP. Unikalność artykułu polega na dokładnym opisie złożonego modelu numerycznego, który przedstawia kroki niezbędne do wykonania kompletnych obliczeń.

Received: 2021-03-05, Revised: 2021-04-22